DRAFT VERSION MARCH 12, 2013
Preprint typeset using LaTeX style emulateapj v. 12/01/06

arXiv:1303.2111v1 [astro-ph.CO] 8 Mar 2013

THE REDSHIFT DISTRIBUTION OF INTERVENING WEAK MgII QUASAR ABSORBERS AND A CURIOUS DEPENDENCE ON QUASAR LUMINOSITY

JESSICA L. EVANS,[1] CHRISTOPHER W. CHURCHILL,[1] MICHAEL T. MURPHY,[2], NIKOLE M. NIELSEN,[1] AND ELIZABETH S. KLIMEK[1]

Draft version March 12, 2013

ABSTRACT

We have identified 469 Mg II $\lambda\lambda 2796, 2803$ doublet systems having $W_r \geq 0.02$ Å in 252 Keck/HIRES and UVES/VLT quasar spectra over the redshift range $0.1 < z < 2.6$. Using the largest sample yet of 188 weak Mg II systems (0.02 Å $\leq W_r < 0.3$ Å), we calculate their absorber redshift path density, dN/dz. We find clear evidence of evolution, with dN/dz peaking at $z \sim 1.2$, and that the product of the absorber number density and cross section decreases linearly with increasing redshift; weak Mg II absorbers seem to vanish above $z \simeq 2.7$. If the absorbers are ionized by the UV background, we estimate number densities of $10^6 - 10^9$ per Mpc^3 for spherical geometries and $10^2 - 10^5$ per Mpc^3 for more sheetlike geometries. We also find that dN/dz toward intrinsically faint versus bright quasars differs significantly for weak and strong ($W_r \geq 1.0$ Å) absorbers. For weak absorption, dN/dz toward bright quasars is $\sim 25\%$ higher than toward faint quasars (10 σ at low redshift, $0.4 \leq z \leq 1.4$, and 4 σ at high redshift, $1.4 < z \leq 2.34$). For strong absorption the trend reverses, with dN/dz toward faint quasars being $\sim 20\%$ higher than toward bright quasars (also 10 σ at low redshift and 4 σ at high redshift). We explore scenarios in which beam size is proportional to quasar luminosity and varies with absorber and quasar redshifts. These do not explain dN/dz's dependence on quasar luminosity.

Subject headings: quasars: absorption lines

1. INTRODUCTION

Quasar absorption line systems are an extremely useful means of statistically constraining the various scenarios of metal enrichment, inflow and outflow, ionization conditions, kinematics, and gas structure within galaxies and the IGM. Various Mg II absorption line studies have concluded that these systems are cosmologically distributed (Lanzetta et al. 1987; Sargent et al. 1988; Steidel & Sargent 1992), and numerous subsequent studies have identified specific galaxies associated with Mg II absorption (see Bergeron & Boissè 1991; Steidel, Dickinson, & Persson 1994; Steidel et al. 1997; Guillemin & Bergeron 1997; Churchill et al. 2005; Chen & Tinker 2008; Kacprzak et al. 2008; Barton & Cooke 2009; Chen et al. 2010; Kacprzak et al. 2011; Churchill et al. 2012; Nielsen et al. 2012).

For the following discussion, we adopt the terms "weak", "intermediate", and "strong" to refer to absorbers having 0.02 Å $\leq W_r < 0.3$ Å, 0.3 Å $\leq W_r < 1.0$ Å, and $W_r \geq 1.0$ Å, respectively, where W_r is the rest frame equivalent width of the Mg II $\lambda 2796$ transition. Mg II-selected gas probes a wide range of H I column density environments. Weak Mg II absorption in particular, which samples optically thin gas over a large span of cosmic time, has been proposed to sample dwarf or LSB galaxies as well as the IGM (Churchill et al. 1999; Rigby et al. 2002). However, there are instances in which weak Mg II is identified in the circumgalactic medium of "normal" bright galaxies (Churchill et al. 2012). Milutinović et al. (2006), using an ionization model, concluded that filamentary and sheetlike IGM structures host at least a portion of weak Mg II absorption. Moreover, Nielsen et al. (2012) argue that $W_r < 0.1$ Å absorbers likely reside in the IGM. Photoionization modeling of weak Mg II systems with associated C IV led Lynch & Charlton (2007) to argue for a scenario of a shell geometry as might be expected for supernova remnants or high velocity clouds moving in a hot corona.

Better insight into the nature of the structures selected by weak Mg II absorbers remains elusive and partially motivates this study. Measurements of the redshift path density dN/dz of weak Mg II absorbers place important constraints on $n(z)\sigma(z)$, the product of their number density and cross section (Churchill et al. 1999; Rigby et al. 2002; Narayanan et al. 2007). In the same vein, probing discrepancies in redshift path densities of Mg II absorption in various equivalent width ranges based on differences in the background sources may reveal information about these absorbing structures. Despite the evidence indicating that absorption line systems are primarily associated with intervening gas as opposed to the background source itself, several studies have nevertheless revealed major discrepancies, depending on the nature of the background source, in the incidence of these absorbers per unit redshift.

Stocke & Rector (1997), in a study of strong Mg II absorbers in BL Lac objects, observed a redshift path density of 4–5 times greater than that expected from quasar surveys. Prochter et al. (2006b) compared quasar and GRB sightlines and found the latter to have a factor of ~ 4 excess in the redshift path density of strong absorbers. A similar study by Vergani et al. (2009) found a factor of ~ 2 excess of strong absorbers, but no excess of intermediate absorbers, in the GRB sample. Bergeron et al. (2011) reported a factor of ~ 2 excess of both strong and intermediate absorbers in blazar versus quasar sightlines. It should be noted, however, that in that study the authors did find marginal statistical evidence in the strong sample of an excess occurring nearer the blazar (even after excluding absorbers having velocity separations of less than 5,000 km s^{-1} from the emission redshift). Finally, in a study analyzing Mg II absorbers down to W_r = 0.07 Å in GRB sightlines, Tejos et al. (2009) found a factor of ~ 3 overabundance of strong absorbers and a $\sim 30\%$ *reduction* for $0.07 \leq W_r < 1.0$ Å compared to studies of quasar sight-

---

[1] New Mexico State University, Las Cruces, NM 88003
[2] Centre for Astrophysics and Supercomputing, Swinburne University of Technology, Hawthorn, Melbourne, VIC 3122, Australia

lines. The latter discrepancy, however, was deemed insignificant since the results were consistent at the 1 σ confidence level. Tejos et al. (2009) have so far presented the only study to compare redshift path density differences in weak Mg II absorbers based on different types of background sources.

In this paper we present the largest study of weak Mg II absorption to date, and for the first time provide a parameterized fit to the redshift path density evolution. We also present our findings of differential absorber redshift path density, based on the absolute magnitude of the background quasar, for weak, intermediate, and strong Mg II systems. In § 2 we present our data, and in § 3 our results. We discuss plausible interpretations in § 4, and conclude in § 5. The cosmological parameters H_0 = 70 km s^{-1} Mpc^{-1}, Ω_m = 0.3, and Ω_Λ = 0.7 are adopted throughout.

2. DATA AND SUBSAMPLES

We have searched 252 Keck/HIRES and UVES/VLT quasar spectra for Mg II $\lambda\lambda2796, 2803$ doublet absorption. All systems were objectively identified using the methods of Schneider et al. (1993) and Churchill et al. (1999). Further details are provided in Evans (2011)[3] and Evans, Churchill & Murphy (2012). The search space omitted redshifts within 5,000 km s^{-1} of the quasar emission redshift, z_{em}, and blueward of the Ly α emission of the quasar. A total of 422 absorbers comprise our sample.

We divided the absorbers into three subsamples using historically motivated weak (Churchill et al. 1999), intermediate (Steidel & Sargent 1992; Nestor et al. 2005), and strong (Steidel & Sargent 1992; Nestor et al. 2005) equivalent width ranges. In order to determine whether our absorber subsamples are consistent with being cosmologically distributed along the lines of sight to the quasars, we performed the second test of Bahcall & Peebles (1969). Performing the Kolmogorov-Smirnov (KS) test for each of our equivalent width ranges, we could not rule out that their distributions are consistent with being cosmological[4]. This result is in agreement with earlier studies (Lanzetta et al. 1987; Sargent et al. 1988; Steidel & Sargent 1992).

Since none of the quasars in our sample were observed with *a priori* knowledge of weak absorption, our survey is unbiased for this population. However, since the quasar sample is drawn from a broad range of targeted science programs, there is the possibility of bias in the intermediate and strong absorbers, which are known to sometimes be associated with DLAs (Rao & Turnshek 2000), or which in some cases were already known due to previous lower resolution surveys.

To examine whether our intermediate and strong absorber samples are consistent with an unbiased population, we compared our measured equivalent width distributions, $f(W_r, W_*)$, where W_* is the characteristic W_r, to the distribution measured by Nestor et al. (2005). Using the KS test for the three redshift bins measured by Nestor et al. (2005), we obtained P(KS) = 0.053 ($0.36 \leq z \leq 0.87$), 0.621 ($0.87 \leq z \leq 1.31$) and 0.322 ($1.31 \leq z \leq 2.27$), respectively. For the full redshift range encompassing all three bins, we obtained P(KS) = 0.115. Even in the case of the lowest value of P(KS), corresponding to the lowest redshift range, the two populations are not inconsistent with each other to even a 2 σ level. We thus proceed under the assumption that our sample of absorbers is a fair sample.

TABLE 1
dN/dz FOR Mg II SURVEYS OF 0.02 Å $\leq W_r <$ 0.3 Å

Survey	$0.4<z<0.7$	$0.7<z<1.0$	$1.0<z<1.4$	$1.4<z<2.4$
CRCV99[a]	1.43 ± 0.21	1.84 ± 0.26	2.19 ± 0.80	···
NMCK07[b]	1.06 ± 0.10	1.51 ± 0.09	1.76 ± 0.08	1.06 ± 0.04
this survey	0.74 ± 0.02	1.08 ± 0.02	0.95 ± 0.02	0.67 ± 0.01

[a] Churchill et al. (1999)
[b] Narayanan et al. (2007)

For our analysis in § 3, we obtained absolute B-band and apparent magnitudes (primarily B, V, and R) of the quasars. The majority were obtained from Veron-Cetty & Veron (2001); 16 were obtained from the NASA/IPAC Extragalactic Database; and for two quasars, the magnitudes could not be determined so these lines of sight and their absorbers were omitted from analysis for which these quantities were required.

3. RESULTS

Following the formalism of Lanzetta et al. (1987), modified to account for the doublet ratio (Churchill et al. 1999), we calculated the number of absorbers per unit redshift, dN/dz.

3.1. *Weak Absorber Redshift Path Density*

For our full redshift range, $0.1 \leq z_{abs} \leq 2.6$, the cumulative redshift path is ΔZ = 231 and is $\sim$ 100% complete to a 5 σ equivalent width sensitivity of $W_r(2796)$ = 0.05 Å and $\sim$ 82% complete to a 5 σ equivalent width sensitivity of $W_r(2796)$ = 0.02 Å. Over the redshift range $0.4 \leq z_{abs} \leq 2.4$, the extent of a study by Narayanan et al. (2007), we have ΔZ = 213, compared to their 70; and for $0.4 \leq z_{abs} \leq 1.4$, the extent of a study by Churchill et al. (1999), we have ΔZ = 148, compared to their 17. These represent the largest two previous weak Mg II surveys. Our larger cumulative redshift path reflects the larger number of lines of sight included in our survey. Churchill et al. (1999) surveyed 26 HIRES quasar spectra and found 30 weak systems, while Narayanan et al. (2007) surveyed 81 UVES quasar spectra and found 112 weak systems. In our survey we identified 188 weak systems.

We calculated dN/dz for weak systems in four redshift bins in order to facilitate comparison with the works of Narayanan et al. (2007) and Churchill et al. (1999); the bins and results are shown in Table 1.

All three studies obtained different results, with the trend being that the dN/dz values have decreased with larger survey size. All three used the identical code (SEARCH, Churchill et al. 1999) for line and candidate identification, and all three ostensibly used the same algorithms in determining the redshift paths for each system. To test for possible differences in the calculations[5], we ran our code used for this survey on the identical spectra and set of systems used by Churchill et al. (1999) and compared their ΔZ and dN/dz results with those of the reproduced study. The result was that the ΔZ values from the Churchill et al. (1999) study were $\sim$ 30% larger than our reproduced values from their data, and the dN/dz values from the original study were thereby lowered compared to our reproduced study. This suggests that our redshift path calculations are more conservative than those of Churchill et al. (1999). If our redshift paths had been calculated exactly as theirs, the dN/dz result of this survey would presumably have been lower, further widening the discrepancy with previous works. A similar duplication of the survey of Narayanan et al. (2007) could not be performed because a significant number of the authors' quasar spectra were unavailable to us.

---

[3] *http://astronomy.nmsu.edu/jlevans/phd*

[4] We calculated the Bahcall & Peebles (1969) Y parameter of each Mg II system, where $0 \leq Y \leq 1$, with Y = 0 representing a doublet at the minimum observed redshift included in the search, and Y = 1 representing a doublet at the maximum observed redshift. Following the formalism of Steidel & Sargent (1992), the sensitivity function $g(Y)$ of the survey was then calculated. This is a measure of the number of lines of sight in the survey in which a system of a given minimum W_r could have been detected at each value of Y. The Y distributions of each absorber sample were then statistically compared to $g(Y)$.

[5] The Churchill et al. (1999) spectra were a subset of the quasars we searched.

In an attempt to find differences in the quasar samples that could possibly lead to the discrepant dN/dz results among the three works, we investigated the quasar apparent magnitude distributions. The KS test was performed between all possible pairs of the three surveys. Our survey and that of Narayanan et al. (2007) exhibit remarkably similar distributions; it could not be ruled out to greater than a 1σ confidence level that their apparent magnitudes had been drawn from the same population, and their median values were both 17.5. In contrast, the Churchill et al. (1999) survey differed from each of the other two to a confidence level of 4σ and had a median apparent magnitude of 16.3. A uniform set of apparent magnitudes in the same band was not available, however, making these comparisons uncertain. The smaller Churchill et al. (1999) survey was undoubtedly overall biased toward brighter quasars.

We likewise investigated the quasar *absolute B*-band magnitude distributions, but when each survey was tested against the other two, it could not be ruled out to even a 1σ confidence level that their distributions had been drawn from the same population. Similarly, no substantial differences were found in the overall median quasar absolute magnitude of the three surveys: −28.5, −28.7, and −28.6 for Churchill et al. (1999), Narayanan et al. (2007), and this study, respectively.

The reasons behind the different dN/dz results among the three works remain unclear; future studies will hopefully resolve the weak Mg II puzzle. It may be that the inclusion or exclusion of weak systems very close to the limiting equivalent width may play a role (Anand Narayanan, private communication), as well as differences in the codes used, since the calculation of ΔZ is extremely sensitive for the weakest systems.

3.2. *Redshift Evolution*

The number of absorbers per unit redshift is the product of the proper number density of absorbers and their proper geometric cross section. In the standard cosmological model, the no-evolution expectation (NEE) for the redshift number density can be parameterized as:

$$\left[\frac{dN}{dz}\right]_{\rm NEE} = \frac{c}{H_0} n_0 \sigma_0 \frac{(1+z)^2}{\sqrt{\Omega_m(1+z)^3+\Omega_\Lambda}} \tag{1}$$

where n_0 is the mean comoving number density of absorbers and σ_0 is the mean comoving geometric absorber cross section. As shown in Figure 1*a*, our observed dN/dz departs strikingly from the NEE (dashed curve), which was normalized to the mean z_{abs}, 1.098, and to the overall dN/dz, 0.83, of our weak sample over the redshift range $0.1 \leq z_{abs} \leq 2.6$. The general behavior of dN/dz is in agreement with Narayanan et al. (2007) in that it peaks between $1.0 < z < 1.4$ and then decreases toward higher redshift.

If the product $n\sigma$ varies as a function of redshift, dN/dz may depart from the no-evolution expectation. The quantity $n(z)\sigma(z)$ can be written as

$$n(z)\sigma(z) = n_0\sigma_0 f(z), \tag{2}$$

where $f(z)$ is a nonnegative function that parameterizes the evolution of dN/dz.

Figure 1*b* depicts our weak dN/dz result divided by the NEE. The data clearly motivate a linear fit; this was achieved using a function of the form

$$f(z) = 1-\alpha(z-z^*), \tag{3}$$

where α is the slope and z^* is the function normalization. The result, $\alpha = 0.69 \pm 0.02$ and $z^* = 1.29 \pm 0.05$, is shown as a solid line in Figure 1*b*.

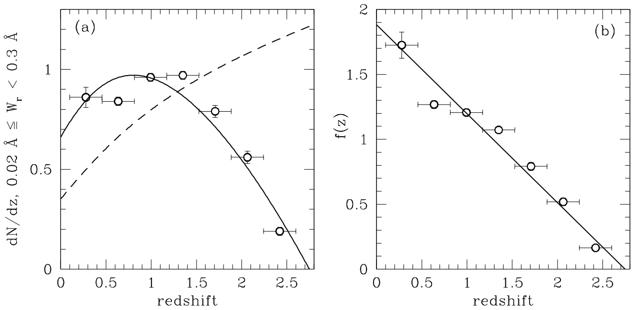

FIG. 1.— (*a*) shows the weak dN/dz (open circles) as well as the NEE (dashed line). — (*b*) shows the same data divided by the NEE. The solid line is the best linear fit to this ratio. In (*a*), this fit was then multiplied by the NEE and plotted (solid curve).

Finally, the fit to $f(z)$ was multiplied by the NEE, yielding a fit to the dN/dz result in Figure 1*a* (solid curve) that can be expressed as

$$\frac{dN}{dz} = \frac{c}{H_0} n_0\sigma_0 \frac{(1+z)^2[1-\alpha(z-z^*)]}{\sqrt{\Omega_m(1+z)^3+\Omega_\Lambda}} \qquad (z < 2.74). \tag{4}$$

Weak Mg II absorbers seem to vanish at high redshift; this result is discussed in § 4.

3.3. *Differential Absorber Redshift Path Densities by Absolute Magnitude*

Motivated by studies that found differences in dN/dz results based on background object as discussed in § 1, as well as our finding of differing apparent magnitude distributions among the weak Mg II studies as discussed in § 3.1, we attempted to discern some intrinsic difference that might affect the observed dN/dz. Using the absolute *B*-band quasar magnitudes of our survey, which had a range of $-32.2 \leq M_B \leq -19.8$, we divided our quasars into "bright" and "faint" subsamples according to the median, $\langle M_B \rangle = -28.6$. The bright subsample has a median of −29.4, and the faint subsample has a median of −27.4.

Figure 2 shows our weak dN/dz results for the bright and faint samples binned as in Figure 1. The redshift path density of the bright sample is clearly higher than that of the faint sample at all redshifts. The lowest redshift bin of the weak bright sample contained only five systems and we believe this caused the dN/dz result in that bin to be less reliable.

Figures 3*a*–3*c* plot our dN/dz results for weak, intermediate and strong Mg II absorption. The bins ($0.4 \leq z_{abs} \leq 1.4$ and $1.4 \leq z_{abs} \leq 2.34$, "low" and "high" redshift) were selected based on previous studies (Narayanan et al. 2007; Nestor et al. 2005; Churchill et al. 1999). Similarly, Figures 3*d*–3*f* show dN/dz calculated for the faint and bright

TABLE 2
dN/dz BY QUASAR LUMINOSITY

sample	weak $0.02 \leq W_r < 0.3$	sig lev	intermediate $0.3 \leq W_r < 1.0$	sig lev	strong $W_r \geq 1.0$	sig lev
			$0.4 \leq z_{abs} \leq 1.4$			
all	0.931 ± 0.006		0.715 ± 0.005		0.449 ± 0.003	
bright	1.040 ± 0.016		0.692 ± 0.010		0.406 ± 0.006	
faint	0.836 ± 0.011		0.730 ± 0.009		0.481 ± 0.006	
bright/all	1.117 ± 0.019	$6.2\ \sigma$	0.967 ± 0.016	$2.1\ \sigma$	0.905 ± 0.015	$6.3\ \sigma$
faint/all	0.897 ± 0.013	$7.9\ \sigma$	1.021 ± 0.014	$1.5\ \sigma$	1.072 ± 0.015	$4.8\ \sigma$
faint/bright	0.803 ± 0.020	$9.9\ \sigma$	1.056 ± 0.019	$2.9\ \sigma$	1.185 ± 0.019	$9.7\ \sigma$
			$1.4 < z_{abs} \leq 2.34$			
all	0.686 ± 0.011		0.696 ± 0.011		0.631 ± 0.010	
bright	0.732 ± 0.018		0.730 ± 0.018		0.584 ± 0.014	
faint	0.579 ± 0.028		0.619 ± 0.030		0.714 ± 0.034	
bright/all	1.068 ± 0.031	$2.2\ \sigma$	1.050 ± 0.031	$1.6\ \sigma$	0.926 ± 0.027	$2.7\ \sigma$
faint/all	0.845 ± 0.043	$3.6\ \sigma$	0.890 ± 0.045	$2.4\ \sigma$	1.131 ± 0.057	$2.3\ \sigma$
faint/bright	0.791 ± 0.054	$3.9\ \sigma$	0.848 ± 0.054	$2.8\ \sigma$	1.222 ± 0.053	$4.1\ \sigma$

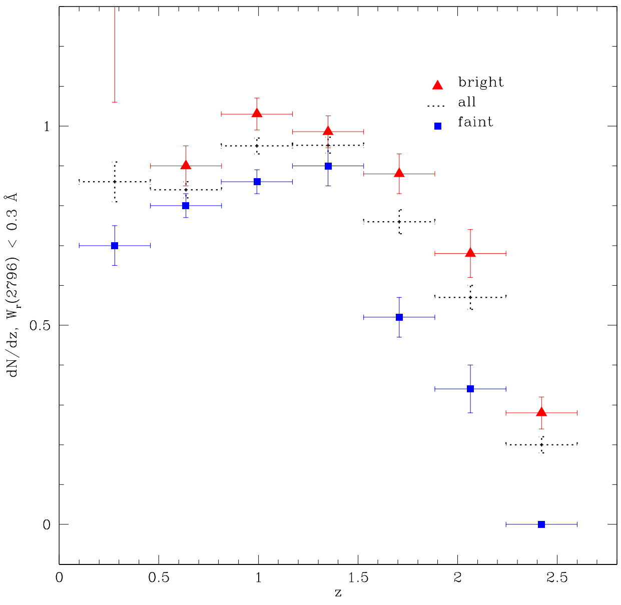

FIG. 2.— dN/dz of the weak sample for the bright (red triangles), faint (blue squares), and combined (dotted crosses) samples. In the bright sample, the lowest redshift data point has a value of 1.53 ± 0.47.

quasar samples. Figures 3*g*–3*i* show the ratio of the dN/dz results of the faint quasar sample to that of the bright. These values are listed in Table 2 for each W_r and redshift range. Though the weak dN/dz results of Churchill et al. (1999), Narayanan et al. (2007), and this study all differed as discussed in § 3.1, the *relative* values among our own faint, bright and all quasar subsamples are robust, having been calculated in a consistent manner. Similarly, though our intermediate and strong samples have W_r distributions consistent with Nestor et al. (2005) as mentioned in § 2, our dN/dz results for these samples are higher than those of Nestor et al. (2005) and Lundgren et al. (2009). This is expected since some of the quasars in our survey were targeted for their known $W_r \geq 0.3$ Å Mg II absorption; however, the dN/dz ratios between our magnitude bins are robust.

For weak systems, the dN/dz values toward bright quasars are $\sim 25\%$ higher than for the faint in both redshift ranges, while for strong systems, dN/dz is $\sim 20\%$ higher toward faint quasars than toward bright in both redshift ranges. The faint to bright dN/dz ratio, $(dN/dz)_f/(dN/dz)_b$, departs for the weak systems from unity at the $\simeq 10\ \sigma$ level for low redshift and at the $\simeq 4\ \sigma$ level for high redshift. The strong absorber ratios are similarly significant (see Table 2), though in that case the faint quasar dN/dz values are higher, rather than lower, than those of the bright sample. In the case of the intermediate absorbers the ratio is consistent with unity within $3\ \sigma$.

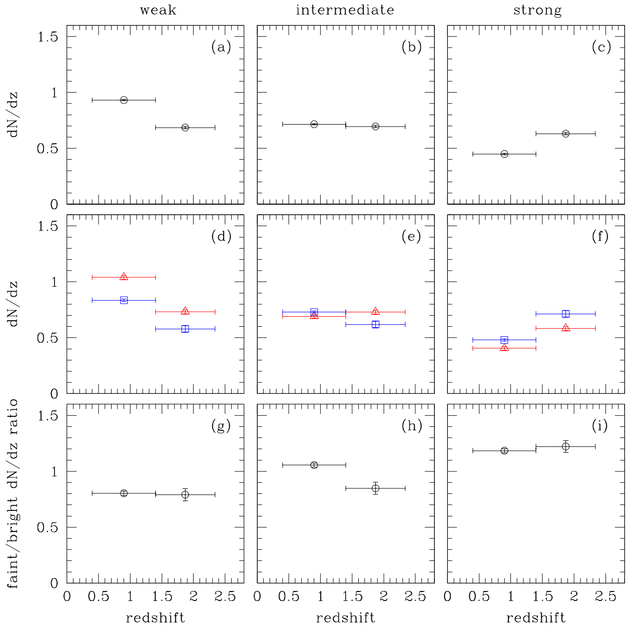

FIG. 3.— (*a*–*c*) show dN/dz of the weak, intermediate and strong samples, respectively, in two redshift bins ($0.4 \leq z_{abs} \leq 1.4$ and $1.4 \leq z_{abs} \leq 2.34$). — (*d*–*f*) show dN/dz for the bright (red triangles) and faint (blue squares) subsamples. The points were left open to better display the error bars. — (*g*–*i*) show the faint to bright dN/dz ratio.

In the calculation of dN/dz the sensitivity of each spectrum is accounted for (see Lanzetta et al. 1987; Evans 2011), eliminating the possibility that the higher values of the weak bright sample compared to the weak faint sample might result from higher signal-to-noise ratios.

4. DISCUSSION

Based on our weak dN/dz result (see Figure 1), the cosmic number density, geometric cross section, or both, of weak Mg II absorbers appear to be evolving. The apparent dropoff in our fit toward $z = 0$ may be overly steep; it is possible that the weak dN/dz peaks at $z \sim 1$, declines slightly and then levels off toward the present. However, it is a first attempt to characterize weak Mg II absorber evolution using a functional form. Our result predicts that no such absorbers exist above $z \simeq 2.7$.

Narayanan et al. (2007) speculated that the apparent paucity of weak Mg II above $z \sim 2$ might be due to the high redshift analogs of low redshift weak Mg II absorption being associated with strong Mg II. In this scenario, weak Mg II absorption at high redshift would be in the kinematic vicinity of strong Mg II and thus would not be recognized as isolated weak absorption. However, we have compared the high velocity weak kinematic subsystems of strong Mg II subsystems to isolated weak Mg II absorption (Evans 2011). Morphologically these two types of profiles often appear very similar, but a KS test of their rest equivalent width distributions revealed that they are actually two distinct populations to a 99.98% confidence level, or greater than 3 σ. A KS test of the distributions of flux decrement-weighted velocity spreads, ω_v (Churchill & Vogt 2001; Evans 2011) indicated to a greater than 6 σ confidence level that the two populations are unique.

The dN/dz evolution we detect in weak Mg II may be due to changes in gas structure or ionization conditions; neither we nor other studies find the same falloff in intermediate and strong Mg II absorption (Nestor et al. 2005; Prochter et al. 2006a; Lundgren et al. 2009) up to our maximum redshift of 2.6. Matejek & Simcoe (2012) do report a decline in the strong population above $z \sim 3$, and note that this peak corresponds to that of the SFR. Our weak dN/dz result, which exhibits no such peak, may provide indirect evidence that a substantial fraction of these absorbers resides in the IGM, since their evolution appears not to correspond to star formation.

Using Cloudy 08.00 photoionization modeling (Ferland et al. 1998), we investigated the evolution of weak Mg II absorber sizes $R(z)$ and cosmic number densities $n(z)$ (for additional details see Evans 2011). In this scenario Mg II selects relatively dense cloudlets embedded within plane parallel slabs of gas. We modeled optically thin clouds having a range of hydrogen number densities based on past Mg II photoionization modeling results (Rigby et al. 2002; Bergeron et al. 2002). We assumed an ultraviolet background model that varies as a function of z, following the work of Haardt & Madau (1996), which includes the contribution of galaxies. Though we examined a grid of clouds with a range of H I column densities and metallicities, we discuss here clouds having $N(\text{H I})$ of 10^{16} cm^{-2} and a metallicity of 0.1 solar. For weak Mg II, $\log N(\text{H I})$ is constrained to the range 15.5–17.0 cm^{-2} (Churchill et al. 2000; Rigby et al. 2002).

The resulting cloud thicknesses, which we interpreted as absorber sizes $R(z)$ and which are governed by the ionizing background, peak at $z \sim 2$ and then decline toward the present, as shown in Figure 4*a*. Assuming spherical clouds, the corresponding absorber cross sections $\sigma(z)$, combined with our weak dN/dz constraint using the fit of Equation 4, translate into cosmic absorber number densities $n(z)$ that increase monotonically toward the present (Figure 4*b*). The absorber sizes produced by this model are on the order of a parsec, and yield absorber number densities on the order of $10^6 - 10^9$ Mpc^{-3}, for the middle range of n_H values. This corresponds to 10^9–10^{12} absorbers per L^* galaxy for $z \lesssim 1$ (Faber et al. 2007) as well as for $1 \lesssim z \lesssim 3$ (Reddy & Steidel 2009; Oesch et al. 2010).

If the clouds are not spherical, but instead the transverse extent R_T scales with cloud thickness according to a factor β such that $R_T = \beta R(z)$, then $n(z)$ would scale as β^{-2}. For $\beta = 100$, $n(z)$ would then be reduced by a factor of 10^4, which yields $10^2 - 10^5$ weak absorbers per Mpc^3. It should be noted that changing the model's $N(\text{H I})$ would change $R(z)$ in direct proportion, while $n(z)$, using our dN/dz constraints, would vary as $N(\text{H I})^{-2}$.

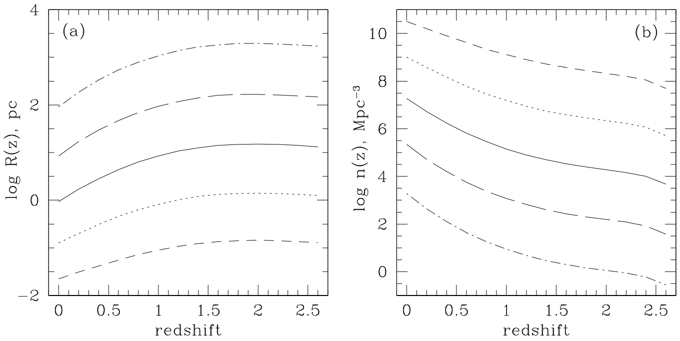

FIG. 4.— (*a*) plots the evolution of Cloudy absorber size, log $R(z)$. (*b*) plots the number density of absorbers, log $n(z)$. The dashed curves represent log n_H = –0.5 cm^{-3}; the dotted curves, log n_H = –1.0 cm^{-3}; the solid curves, log n_H = –1.5 cm^{-3}; the long dashed curves, log n_H = –2.0 cm^{-3}; and the dashed-dotted curves, log n_H = –2.5 cm^{-3}.

Our Cloudy model is suggestive of a condensation mechanism into sheet or filament structures characteristic of the IGM. Sheetlike geometries require far fewer weak absorbers than do spherical geometries per L^* galaxy, and therefore we consider these to be a more realistic scenario. Although we do not fully explain the nature of weak Mg II absorption, this exercise does provide a limiting case in which to couch the phenomenon. Our absorber size estimate is not far from that of Rigby et al. (2002), who concluded that a sheetlike structure containing many embedded $\sim$ 10 pc absorbers was required to account for the observed dN/dz. Recent findings by Churchill et al. (2012) and Nielsen et al. (2012) indicate that $0.1 \leq W_r \leq 0.3$ Å, but not $0.02 \leq W_r \leq 0.1$ Å, absorbers are found in the circumgalactic medium of normal galaxies at impact parameters of less than 200 kpc. They suggest that the weaker of these two populations may then reside primarily in the IGM.

Our dN/dz results toward faint versus bright absolute magnitude quasars reveal that the weak absorbers have a higher redshift path density in the bright quasar sample than in the faint at both low and high redshifts. For the strong absorbers, the opposite is true. The intermediate absorbers appear to follow no clear trend, and may represent an equivalent width range where the effects leading to the weak and strong differentials mostly cancel.

Following the discovery by Prochter et al. (2006b) of the quasar–GRB strong Mg II discrepancy, various researchers have attempted to explain the phenomenon. Frank et al. (2007) modeled the effects of Mg II absorber size and impact parameter on observed equivalent width and concluded that the dN/dz discrepancy may be due to the larger beam sizes of quasars versus GRBs, the latter of which they state are on the order of the sizes of cloud cores. The authors also predicted that different luminosity populations of quasars should contain different incidences and strengths of intervening absorbers.

Porciani et al. (2007) countered this differential beam size argument, noting that no unsaturated Mg II doublets have been observed having a doublet ratio of one, as would be expected in the case of partial covering of a quasar beam by an absorber. They stated that magnification bias could explain the discrepancy, and that dust obscuration bias and association of absorbers with the circumburst environment could also partially account for it.

A statistical study was also conducted by Pontzen et al. (2007) to look for systematically lowered Mg II equivalent widths over quasar broad line emission regions, which are substantially larger than quasar continuum regions; no significant difference was found.

Cucchiara et al. (2009) cite an intrinsic origin as a possible explanation for the GRB excess. Mg II absorbing gas could be ejected at relativistic velocities and masquerade as an intervening absorber; however, the authors note that the presence of Mg I absorption in these systems, as well as the lack of fine structure transitions that are expected in the vicinity of a GRB, cast doubt on this theory. Vergani et al. (2009) concur that the excess could be intrinsic, and estimate required ejection velocities of $10,000-25,000$ km s^{-1}. They also consider gravitational lensing to be a viable mechanism to account for the discrepancy.

In two studies of C IV absorbers toward GRBs, Sudilovsky et al. (2007) and Tejos et al. (2007) reported no excess incidence over quasar sightlines. Sudilovsky et al. (2007) speculated that the difference in the cases of Mg II versus C IV absorbers arose partially because the former introduced more dust extinction than the latter. However, dust extinction in Mg II absorbers was subsequently modeled (Sudilovsky et al. 2009), and the authors concluded that the effect could only account for $\sim 10\%$ of the quasar–GRB discrepancy.

Tejos et al. (2009) rejected an intrinsic origin for excess GRB Mg II absorbers due to the lack of both excess C IV absorption and excess weak and intermediate Mg II absorption, and instead favored gravitational lensing as the relevant mechanism. Wyithe et al. (2011) modeled gravitational lensing in quasar and GRB sightlines and concluded that it was a feasible explanation for the excess, but that further GRB data were necessary to support or refute their findings. They noted that afterglows in which strong Mg II systems are found are brighter than average, implying a greater lensing rate.

Through their modeling of extinction curves toward quasars and GRBs, Budzynski & Hewett (2011) determined that dN/dz toward quasars would be significantly higher if corrected for dust, and that the correction varies with redshift. The discrepancy compared to GRBs arises, the authors state, because their absorber redshift distribution is shifted higher than that of quasars, resulting in less loss of detected absorbers. They calculated that this effect could account for a factor of two excess in the GRB dN/dz.

Keeping these previous studies of the quasar–GRB discrepancy in mind, and in an attempt to understand the possibly related phenomenon we have uncovered, we attempted to find some other metric within our faint and bright quasar samples that would shed light on these issues. The redshift path density depends on the integrated equivalent width distribution,

$$\frac{dN}{dz} \propto \int_{W_{min}}^{W_{max}} f(W, W_*)\, dW\,. \tag{5}$$

We therefore compared equivalent width distributions for our faint and bright quasar samples for the various W_r ranges as well as for low, high, and all redshifts.

We also studied equivalent width distributions binned by relative beam sizes using M_B as a proxy, i.e. assuming that the square of the source radius R_s is proportional to the B-band luminosity of the quasar. The ratio of the source radius for quasar i relative to the median radius for the full quasar sample can then be written (Shakura & Sunyaev 1973) as

$$\frac{R_{s,i}}{\langle R_s \rangle} = 10^{-0.2(M_i - \langle M_B \rangle)}. \tag{6}$$

We then studied the effect of changing beam size with redshift due to cosmology. We calculated the ratio of the relative beam size of quasar i at the redshift of absorber j to the cross section of the source:

$$\frac{\sigma_b(z_j)}{\sigma_{s,i}} = \left[\frac{D_A(z_j)}{D_A(z_{s,i})} \right]^2 \tag{7}$$

where $\sigma_{s,i} = \pi R_{s,i}^2$, $D_A(z_j)$ is the angular diameter distance at the absorption redshift of system j, and $D_A(z_{s,i})$ is the angular diameter distance at the source redshift of quasar i. Finally, we examined the combined effect of source size and cosmology, by using Equation 6 to scale σ_b.

Using the KS test, none of these equivalent width distributions yielded significant differences (of at least 3 σ) between the faint and bright quasar samples. Since the dN/dz discrepancy is in this case of a smaller magnitude than in the case of the quasar–GRB phenomenon, it may require a larger data set to discern the reasons behind the observations.

The findings of Budzynski & Hewett (2011) do offer an intriguing possibility by relating absorption redshift distributions to dN/dz. Our faint absorber samples do have lower median z_{abs} values than our bright samples across all three equivalent width ranges, probably a result of the correlation whereby intrinsically more luminous quasars tend to be selected at higher redshifts. This result only supports the authors' dust argument in the case of our weak absorbers, the only sample in which the absorption incidence is significantly higher toward bright quasars than faint. For our weak sample, the median absorption redshift is 0.87 in the faint subsample and 1.17 in the bright. KS testing, however, revealed that it could not be ruled out to a greater than 98.32% confidence level that the faint and bright subsamples are drawn from the same underlying z_{abs} distribution.

Though several authors have argued for an intrinsic origin for excess strong Mg II absorption toward GRBs versus quasars, this does not appear to explain the dN/dz discrepancy in the case of our bright and faint quasar populations. Our Bahcall & Peebles (1969) testing revealed absorber distributions consistent with cosmological within all equivalent width and quasar absolute magnitude subsamples, as well as in the aggregate populations. The velocities of Mg II-selected gas ejected from a quasar would have to reach large fractions of the speed of light in order to pass for intervening systems. It therefore seems highly unlikely that significant intrinsic absorption could be present in our sample.

5. CONCLUSION

We have found in a survey of 252 quasar spectra that the incidence of weak Mg II absorption evolves markedly, that it peaks at $z \sim 1.2$, and that it is fit by a function that is a product of the no-evolution expectation with a linear function. Our linear fit to the ratio of our dN/dz data to the NEE resulted in a slope of $\alpha = 0.69 \pm 0.02$ and a normalization of $z^* = 1.29 \pm 0.05$ for the function $f(z) = 1 - \alpha(z - z^*)$. Our dN/dz result predicts that no weak Mg II absorbers exist above $z \simeq 2.7$.

We find that when our quasar survey is segregated by absolute magnitude, weak Mg II dN/dz is significantly lower in the faint subsample than in the bright, with faint to bright dN/dz ratios of 0.80 ± 0.02 at low redshift and 0.79 ± 0.05 at high redshift. In contrast, strong Mg II dN/dz is significantly *higher* in the faint subsample than in the bright, with faint to bright dN/dz ratios of 1.19 ± 0.02 at low redshift and 1.22 ± 0.05 at high redshift. Intermediate equivalent width absorbers exhibited dN/dz ratios consistent with unity within 3 σ. At this time it is uncertain whether these results stem from some intrinsic property of the quasars, from some difference in the intervening sightlines, or from some combination of these factors.

We thank Wallace Sargent, Michael Rauch, Jason Prochaska, and Charles Steidel for their contribution of spectra, and Anand Narayanan for helpful communications regarding Narayanan et al. (2007). This research made use of the NASA/IPAC Extragalactic Database (NED), which is operated by the Jet Propulsion Laboratory, California Institute of Technology, under contract with NASA. We are grateful for NSF grant AST 0708210, the primary funding for this work; JLE was also supported by a three-year Aerospace Cluster Fellowship administered by the Vice Provost of Research at New Mexico State University and by a two-year New Mexico Space Grant Graduate Research Fellowship. MTM thanks the Australian Research Council for a QEII Research Fellowship (DP0877998).

REFERENCES

Bahcall, J. N., & Peebles, P. J. E. 1969, ApJ, 156, L7

Barton, E. J., & Cooke, J. 2009, AJ, 138, 1817

Bergeron, J., Aracil, B., Petitjean, P., & Pichon, C. 2002, A&A, 419, 811

Bergeron, J., & Boissè, P. 1991, å, 243, 334

Bergeron, J., Boissé, P., & Ménard, B. 2011, A&A, 525, 51

Budzynski, J. M., & Hewett, P. C. 2011, MNRAS, 416, 1871

Chen, H.-W., Helsby, J. E., Gauthier, J.-R., Shectman, S. A., Thompson, I. B., & Tinker, J. L. 2010, ApJ, 714, 1521

Chen, H.-W., & Tinker, J. L. 2008, ApJ, 687, 745

Churchill, C. W., Kacprzak, G. G., Nielsen, N. M., Steidel, C. C., & Murphy, M. T. 2012, ApJ, submitted

Churchill, C. W., Kacprzak, G. G., & Steidel, C. C. 2005, IAU Colloq. 199: Probing Galaxies through Quasar Absorption Lines, 24

Churchill, C. W., Rigby, J. R., Charlton, J. C., & Vogt, S. S. 1999, ApJS, 120, 51

Churchill, C. W., Mellon, R. R., Charlton, J. C., Jannuzi, B. T., Kirhakos, S., Steidel, C. C., & Schneider, D. P. 2000, ApJS, 130, 91

Churchill, C. W., & Vogt, S. S. 2001, ApJ, 122, 679

Cucchiara, A., Jones, T., Charlton, J. C., Fox, D. B., Einsig, D., & Narayanan, A. 2009, ApJ, 697, 345

Evans, J. L. 2011, Ph.D. thesis, New Mexico State University

Evans, J. L., Churchill, C. W., & Murphy, M. T. 2012, ApJS, in preparation

Faber, S. M. et al. 2007, ApJ, 665, 265

Ferland, G. J., Korista, K. T., Verner, D. A., Ferguson, J. W., Kingdon, J. B., & Verner, E. M. 1998, PASP, 110, 761

Frank, S., Bentz, M. C., Stanek, K. Z., Mathur, S., Dietrich, M., Peterson, B. M., & Atlee, D. W. 2007, Ap&SS, 312, 325

Guillemin, P., & Bergeron, J. 1997, å, 328, 499

Haardt, F., & Madau, P. 1996, ApJ, 461, 20

Kacprzak, G. G., Churchill, C. W., Evans, J. L., Murphy, M. T., & Steidel, C. C. 2011, MNRAS, 416, 3118

Kacprzak, G. G., Churchill, C. W., Steidel, C. C., & Murphy, M. T. 2008, AJ, 135, 922

Lanzetta, K. M., Turnshek, D. A., & Wolfe, A. M. 1987, ApJ, 332, 739

Lundgren, B. F., Brunner, R. J., York, D. G., Ross, A. J., Quashnock, J. M., Myers, A, D., Schneider, D. P., Al Sayyad, Y., & Bahcall, N. 2009, ApJ, 698, 819

Lynch, R. S., & Charlton, J. C. 2007, ApJ, 666, 64

Matejek, M. S., & Simcoe, R. A. 2012, ApJ, submitted

Milutinović, N., Rigby, J. R., Masiero, J. R., Lynch, R. R., Palma, C., Charlton, J. C. 2006, ApJ, 641, 190

Narayanan, A., Misawa, T., Charlton, J. C., & Kim, T. 2007, ApJ, 660, 1093

Nestor, D. B., Turnshek, D. A., & Rao, S. M. 2005, ApJ, 628, 637

Nielsen, N. M., Churchill, C. W., & Kacprzak, G. G. 2012, ApJS, in preparation

Oesch, P. A., Bouwens, R. J., Carollo, C. M., Illingworth, G. D., Magee, D., Trenti, M., Stiavelli, M., Franx, M., Labbé, I., & van Dokkum, P. G. 2010, ApJ, 725, 150

Pontzen, A., Hewett, P., Carswell, R., & Wild, V. 2007, MNRAS, 381, 99

Porciani, C., Viel, M., & Lilly, S. J. 2007, ApJ, 659, 218

Prochter, G. E., Prochaska, J. X., & Burles, S. M. 2006a, ApJ, 639, 766

Prochter, G. E., Prochaska, J. X., Chen, H., Bloom, J. S., Dessauges-Zavadsky, M., Foley, R. J., Lopez, S., Pettini, M., Dupree, A. K., & Guhathakurta, P. 2006b, ApJ, 648, 93

Rao, S. M., & Turnshek, D. A. 2000, ApJS, 130, 1

Reddy, N.A., & Steidel, C. C. 2009, ApJ, 692, 778

Rigby, J. R., Charlton, J. C., & Churchill, C. W. 2002, ApJ, 565, 743

Sargent, W. L. W., Steidel, C. C., & Boksenberg. A. 1988, ApJ, 334, 22

Schneider, D. P., et al. 1993, ApJS, 87, 45

Shakura, N. I., & Sunyaev, R. A. 1973, A&A, 24, 337

Steidel, C. C., Dickinson, M., Meyer, D. M., Adelberger, K. L., & Sembach, K. R. 1997, ApJ, 480, 586

Steidel, C. C., Dickinson, M., & Persson, S. E. 1994, ApJ, 437, L75

Steidel, C. C., & Sargent, W. L. W. 1992, ApJS, 80, 1

Stocke, J. T., & Rector, T. A. 1997, ApJ, 489, 17

Sudilovsky, V., Savaglio, S., Vreeswijk, P., Ledoux, C., Smette, A., & Greiner, J. 2007, ApJ, 669, 741

Sudilovsky, V., Smith, D., & Savaglio, S. 2009, ApJ, 699, 56

Tejos, N., Lopez, S., Prochaska, J. X., Bloom, J. S., Chen, H., Dessauges-Zavadsky, M., Maureira, M. J. 2009, ApJ, 706, 1309

Tejos, N., Lopez, S., Prochaska, J. X., Chen, H., & Dessauges-Zavadsky, M. 2007, ApJ, 671, 622

Vergani, S. D., Petitjean, P., Ledoux, C., Vreeswijk, P., Smette, A., Meurs, E. J. A. 2009, å, 503, 771

Veron-Cetty, M. P., & Veron, P. 2001, A&A, 374, 92

Wyithe, J. S. B., Oh, S. P, & Pindor, B. 2011, MNRAS, 414, 209